Rapid Communications

Zeeman-driven superconductor-insulator transition in strongly disordered MoC films: Scanning tunneling microscopy and transport studies in a transverse magnetic field

M. Žemlička,[1,3,4] M. Kopčík,[1,5] P. Szabó,[1] T. Samuely,[2] J. Kačmarčík,[1] P. Neilinger,[3] M. Grajcar,[3] and P. Samuely[1,2]

[1]*Centre of Low Temperature Physics, Institute of Experimental Physics, Slovak Academy of Sciences, 04001 Košice, Slovakia*
[2]*Centre of Low Temperature Physics, Faculty of Science, P. J. Šafárik University, 04001 Košice, Slovakia*
[3]*Department of Experimental Physics, Comenius University, 84248 Bratislava, Slovakia*
[4]*Institute of Science and Technology Austria, am Campus 1, 3400 Klosterneuburg, Austria*
[5]*Faculty of Electrical Engineering and Informatics, Technical University, 04001Košice, Slovakia*

(Received 17 March 2020; revised 5 June 2020; accepted 4 November 2020; published 23 November 2020; corrected 20 September 2021)

The superconductor-insulator transition in a transverse magnetic field is studied in a highly disordered MoC film with the product of the Fermi momentum and the mean free path $k_F l$ close to unity. Surprisingly, the Zeeman paramagnetic effects dominate over orbital coupling on both sides of the transition. In the superconducting state it is evidenced by a high upper critical magnetic field B_{c2}, by its square-root dependence on temperature, as well as by the Zeeman splitting of the quasiparticle density of states (DOS) measured by scanning tunneling microscopy. At B_{c2} a logarithmic anomaly in DOS is observed. This anomaly is further enhanced in an increasing magnetic field, which is explained by the Zeeman splitting of the Altshuler-Aronov DOS driving the system into a more insulating or resistive state. A spin-dependent Altshuler-Aronov correction is also needed to explain the transport behavior above B_{c2}.

DOI: 10.1103/PhysRevB.102.180508

Two-dimensional (2D) superconductors can be driven through a quantum superconductor-insulator transition (SIT) by tuning various physical parameters, such as disorder, voltage gating, or magnetic field [1,2]. In general, two principal mechanisms of SIT exist. In the bosonic scenario, the phase coherence of the Cooper-pair condensate is disrupted, and puddles with a variant superconducting order parameter emerge and survive even on the insulating side [3,4]. In the fermionic scenario [5], the amplitude of the superconducting order parameter is fully suppressed, driving the superconducting transition temperature to zero. Our previous papers demonstrated that increased disorder in ultrathin MoC films leads to the fermionic scenario of the suppression of superconductivity [6,7].

Recently, the exclusivity of the insulating ground state in 2D superconductors after a quantum transition has been called into question. A quantum superconductor-(anomalous) metal transition was suggested as a viable alternative [8,9]. In this Rapid Communication, it is impossible to distinguish these two options, due to finite temperatures. Hence, for the sake of clarity, we will address the effects simply as SIT in the following.

Here, we use another SIT control parameter—a magnetic field oriented perpendicularly to an ultrathin MoC film. The external magnetic field interacts with electrons via two different mechanisms: Zeeman and orbital couplings. For perpendicular fields, usually the latter mechanism is dominant. In our study, counterintuitively, in addition to orbital coupling, Zeeman coupling also plays an important role in the superconducting as well as the insulating/normal state. It is evidenced by a high upper critical magnetic field B_{c2}, by its square-root dependence on temperature, as well as by the Zeeman splitting of the superconducting quasiparticle density of states (DOS) measured by scanning tunneling microscopy (STM). This surprising finding is related to the fact that the spin pair breaking is comparable to the orbital one, since the product of the Fermi wave number and mean free path, known as the Ioffe-Regel parameter $k_F l$, is close to unity. In magnetic fields above B_{c2} a logarithmic anomaly in the density of states due to the Altshuler-Aronov effect of 2D disordered metals [10,11] is present. Surprisingly, the anomaly is enhanced in a further increasing magnetic field driving the system deeper into an insulating/resistive state. This effect is also explained as a consequence of the Zeeman effect, and now on the Altshuler-Aronov DOS. A Zeeman spin-dependent Altshuler-Aronov correction is also needed to describe the temperature dependence of sheet resistances at low temperatures in fields above B_{c2}, strongly supporting the Zeeman-driven SIT in a transverse magnetic field in MoC.

MoC films of 3-nm thickness were prepared by reactive magnetron sputtering onto a Si substrate as described in Refs. [12,13]. The Ioffe-Regel parameter $k_F l$ was determined for all our thin MoC films [6,12] from the free-electron model. Transport and STM measurements were performed in magnetic fields up to 16 and 8 T, respectively, all at temperatures down to 0.3 K. Details are given in the Supplemental Material [14].

Strongly disordered ultrathin MoC films reveal quantum corrections to Drude conductivity with a negative temperature derivative of the sheet resistance $dR_\square/dT$ from room temperatures down to the superconducting transition [6].

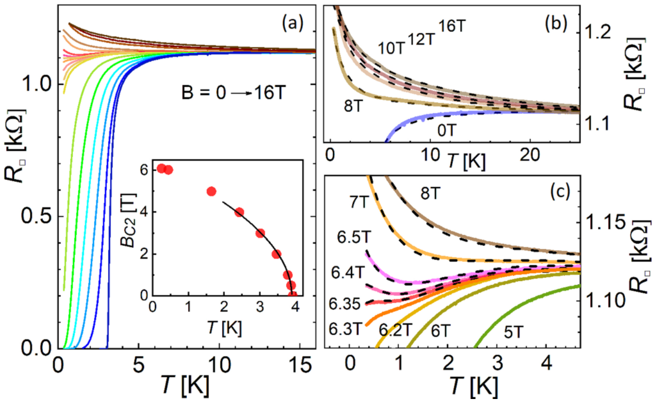

FIG. 1. (a) Temperature dependence of the sheet resistance of MoC film at magnetic fields $B = 0$, 1, 2, 3, 4, 5, 6, 6.2, 6.3, 6.35, 6.4, 6.5, 7, 8, 10, 12, and 16 T. The inset shows the temperature dependence of $B_{c2}(T)$ determined from resistive transitions (symbols). The solid black line is a $B_{c2}(T) \propto \sqrt{T_c - T}$ fit at $T \rightarrow T_c$. (b) and (c) show details of the resistive transitions, and dashed black lines are fits (see the main text and Supplemental Material [14])

Figure 1(a) shows $R_\square(T)$ up to 16 T. At zero field a broad superconducting transition is observed due to superconducting fluctuations typical for disordered 2D systems. In a magnetic field the initial drop of resistance is moving to lower temperatures and the transitions are further broadened. More details can be viewed in Figs. 1(b) and 1(c). In the field range 6.2–7 T, the slope of $R_\square(T)$ exhibits nonmonotonous behavior. The onset of superconductivity is followed by a kink or minimum, and the 6.2-, 6.3-, and 6.35-T curves exhibit a superconducting reentrant behavior with a second downturn of the $R_\square(T)$. Above 6.4 T no sign of reentrant superconductivity is observed, indicating that the value is already above the upper critical field B_{c2}. At $B > 7$ T the slope of $R_\square(T)$ resumes the monotonous behavior in the whole temperature range with an insulatorlike negative derivative $dR_\square/dT$ up to our highest field of 16 T. The inset of Fig. 1(a) shows the temperature dependence of $B_{c2}(T)$ determined at 90% of the "normal-state" sheet resistance $R^N_\square(15\text{ K}) = 1120\ \Omega$ (symbols) with a negative curvature that can be described by a $B_{c2}(T) \propto \sqrt{T_c - T}$ formula (solid line). Such a curvature is typical for the critical field in paramagnetic limit B^P [15], where pair breaking is caused by Zeeman splitting. See also the Supplemental Material [14].

The temperature dependence $R_\square(T)$ above $B_{c2} \sim 6.3$ T was fitted by the sum of the Drude conductivity, the contribution of superconducting fluctuations in the Cooper channel [11,16,17], and the Altshuler-Aronov correction in the diffusion channel [10,11]. As discussed in detail in the Supplemental Material [14], a successful fit of the data is obtained only when the spin-splitting effects are taken into account, indicating that not only orbital but also the Zeeman effect is at play in the transverse magnetic field. Our tunneling experiments provide more conclusive arguments for a Zeeman-driven SIT.

Figure 2(a) displays typical tunneling spectra as a function of temperature. At the lowest temperature $T = 0.5$ K the spectrum shows reduced coherence peaks and in-gap states for which thermal smearing alone cannot account. Upon a temperature increase the gap closes with the in-gap states growing and the coherence peaks ceasing. Above $T_c = 3.95$ K no superconducting features are visible. Still, the tunneling conductance shows a slight increase with the absolute value of voltage. The overall temperature dependence can be described within the thermally smeared Dynes DOS, $N_S^D(E) = (E + i\Gamma_D)/\sqrt{(E + i\Gamma_D)^2 - \Delta^2}$, with the superconducting gap Δ and the parameter Γ_D responsible for spectral broadening [18,19]. The fitting curve at $T = 0.5$ K is plotted as a black solid line in Fig. 2(a). The temperature dependence of the energy gap determined from the fit follows the BCS prediction with $\Delta(0) = 0.65$ meV, $\Gamma_D = 0.25$ meV, $T_c = 3.95$ K, and $2\Delta/k_BT_c = 3.8$, in agreement with our previously published results [6,7]. The gapless superconducting DOS described by the Dynes modification of the BCS DOS [18] has been recently microscopically explained by the presence of local pair-breaking fields at arbitrary potential disorder [19]. In MoC such pair-breaking fields are formed at the interface between the substrate and the film [7].

Figure 2(b) shows an effect of perpendicular magnetic field on the tunneling spectra at $T = 0.5$ K. When B is increased, the superconducting gap is gradually filled, and the coherence peaks are smeared. Notably, the gap structure of the tunneling spectra is not fully suppressed when B_{c2} is approached, but the tunneling conductance measured above $B_{c2} \sim 6.3$ T still shows a minimum at the zero-bias voltage.

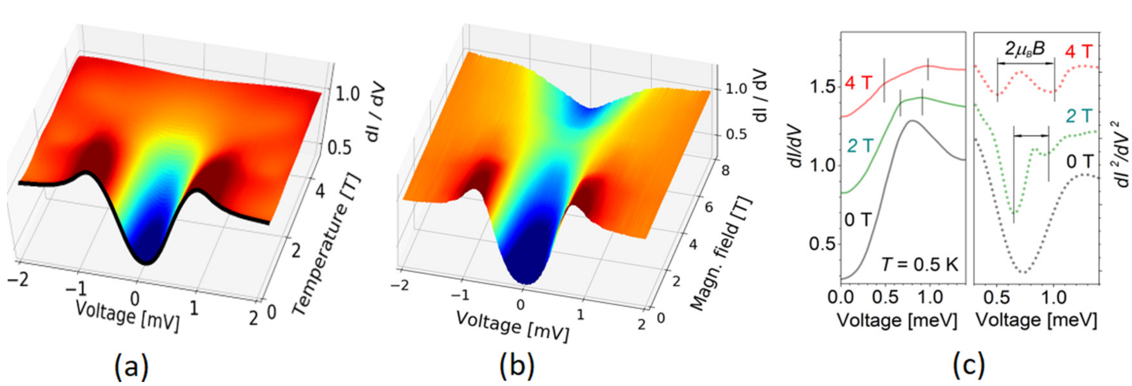

FIG. 2. (a) Temperature dependence of the STM differential conductance spectra in zero field. The black curve is a Dynes fit. (b) Magnetic field dependence of the spectra at 0.5 K. (c) Left: The spectra taken at $B = 0\,T$ (black), 2 T (green), and 4 T (red) magnetic fields with smeared Zeeman splitting features. Right: The second derivative of the spectra from the left panel. For a description, see the main text.

Astonishingly, this feature is enhanced by further increasing the field above B_{c2}. It is noteworthy that this effect is uniform across the sample surface, in contrast to the superconducting features as shown in the conductance maps of Fig. S1 in the Supplemental Material [14]. It indicates that the spectra taken above 6.3 T do not reflect the superconducting DOS but rather the normal-state properties without any spatial variations.

Figure 2(c) displays a rare case of superconducting spectra with a smaller broadening parameter Γ_D. In magnetic fields of 2 and 4 T this smearing enables the observation of two faint kinks marked by vertical bars. The effect is better resolved in the second derivative of the tunneling conductance d^2I/dV^2, where a pair of distinct minima is present. The distance between the minima is equal to $2\mu_B B$, consistent with Zeeman spin splitting.

Zeeman spin-splitting and orbital pair-breaking effects are characterized by their respective critical magnetic fields. In a dirty type-II superconductor the orbital upper critical field $B_{c2} \sim \Phi_0/(\xi_0 l)$, where Φ_0 is the flux quantum and $\xi_0 = \hbar v_F/\pi\Delta$ is the BCS coherence length. Due to the Zeeman coupling, the Cooper pairing would be destroyed by the Pauli depairing field $B^P \sim \Delta/\mu_B$, where μ_B is the Bohr magneton.

The ratio between these fields is $B^P/B_{c2} \sim k_F l$ showing that in materials which are close to SIT the Zeeman and orbital couplings are similar. The dominance of the Zeeman splitting of strongly interacting electrons was observed at the metal-insulator transition in disordered metals (e.g., the case of Si:B [20]). We assume that this effect can dominate also in superconductors near SIT. In the case of Zeeman splitting the spin-up and spin-down states in superconducting DOS are separated by $2\mu_B B \approx 0.116B$ (meV) in magnetic field B and the gap peak splits in two [21]. It is documented in Fig. 2(c) by the weakly smeared spectrum where the inequality $\Delta > \mu_B B > \Gamma_D$ holds.

It was shown in Ref. [19] that in Dynes superconductors the first-order phase transition at the Zeeman-driven critical magnetic field transforms into a continuous transition when Γ_D exceeds $\sim 0.3\Delta(0)$. Still, there is a characteristic response to the magnetic field in tunneling DOS. While in the case of orbital pair breaking the separation of the gap peaks shrinks, at Zeeman coupling the distance between the gaplike peaks remains nearly constant up to B^P. This means that gap filling rather than gap closing with increasing B should be observed. Our MoC films are indeed Dynes superconductors [7,19] with spectral broadening in the range $\Gamma_D = 0.25\Delta$–0.36Δ. High spectral broadening in most of our spectra washes out the Zeeman splitting signatures, leaving just a broadened gap maximum. Still, one can observe in Fig. 3(a) that the gap-peak position remains almost unchanged upon increasing B up to B_{c2} (dashed lines crossing the green curves), consistent with Zeeman coupling.

Thus, for a 3-nm MoC film in the superconducting state, the effect of a transverse magnetic field on the tunneling DOS, the square-root temperature dependence of the upper critical field, and its magnitude $B_{c2}(0) \sim 6.3$ T in the range of the Clogston limit [$B^P(\mathrm{T}) \simeq 1.8T_c$ (K) [22]] is evidence of the paramagnetic Cooper-pair breaking. Above B_{c2} the Altshuler-Aronov anomaly in DOS is further enhanced by the magnetic field.

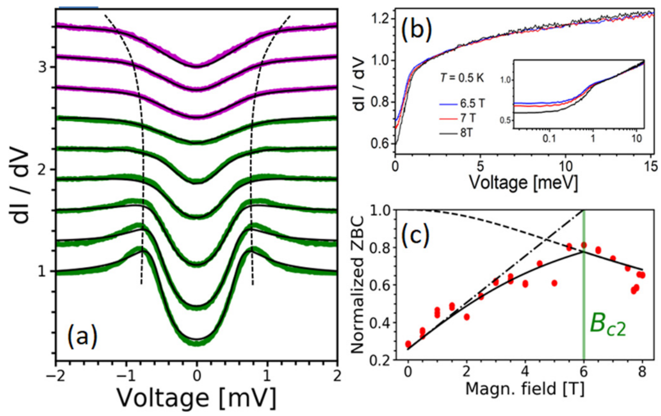

FIG. 3. (a) Tunneling spectra from Fig. 2(b) in magnetic fields $B = 0, 0.5, 2, 3, 4, 6$ (superconducting state, green color) and at 6.5, 7, and 8 T (normal state, magenta) fitted to the model (black lines) described in the text. The dashed lines follow the field dependence of the superconducting gap maxima and the smeared Zeeman singularity positions. (b) Tunneling spectra at $T = 0.5$ K and $B = 6.5$, 7, and 8 T (blue, red, black lines) measured in a voltage window (0, +15 mV). The inset of (b) is the logarithmic plot of the same curves. (c) Magnetic field dependence of the zero-bias conductance (red symbols) compared to theoretical models (dashed line: Altshuler-Aronov effect; dashed-dotted line: Dynes model; solid line: linear combination of the models).

In Fig. 3(b) the normal-state tunneling conductance taken at $B = 6.5$, 7, and 8 T fields is displayed in a wider voltage range. The inset plots the curves in a logarithmic scale. All the spectra reveal the same logarithmic energy dependence down to ≈ 1 meV, where an abrupt field-dependent change occurs. In an increased magnetic field the position of the change shifts slightly to higher energies and the zero-bias conductance (ZBC) decreases, similarly as in Fig. 2(b).

It is well established that strong disorder enhances the electron-electron interaction. According to the Altshuler-Aronov (AA) theory of 2D systems [10,11], this is manifested by a logarithmic suppression of the DOS near the Fermi level at energies $k_B T \ll E \ll \Gamma$, where $\Gamma = \hbar/\tau \sim 10$ eV, inversely proportional to the short mean free time τ in strongly disordered systems, is much greater than other relevant energy scales [23]. In our case the DOS starts to saturate at approximately 0.3 meV. This value is one order of magnitude higher than the thermal energy $k_B T = 0.043$ meV at $T = 0.5$ K, but is very close to the spectral broadening as discussed below.

Now we turn to the effect of magnetic field on the tunneling spectra above B_{c2}. The standard AA correction is field independent, but taking the electron spins into account in the diffusive particle-hole channel leads to a field dependence of the correction to the normalized DOS, $N_N(E) = 1 - \delta\tilde{N}$. In the presence of finite relaxation rates, it can be derived from Eq. (6.2a) in Ref. [11] as

$$\widetilde{\delta N}(E,T,B) = \chi\Bigg\{f(\tilde{E},\tilde{\Gamma}_0) + \frac{\lambda_1}{2\lambda_0}\Bigg[f(\tilde{E},\tilde{\Gamma}_1) + \frac{1}{2}\sum_{\alpha=\pm 1} f(\tilde{E}+\alpha\tilde{E}_Z,\tilde{\Gamma}_1)\Bigg]\Bigg\}, \quad (1)$$

where arguments of the function f are normalized to the thermal energy as, e.g., the Zeeman energy $\tilde{E}_Z = 2\mu_B B/k_B T$. The function f is defined as

$$f(a,b) = -\frac{1}{2}\int_0^{\Gamma/k_BT} dx \frac{x}{x^2+b^2}\frac{\sinh(x)}{\cosh(x)+\cosh(a)}.$$

The parameter χ includes constants as parameters of the tunneling barrier and the constant uncorrected density of states. The constants of λ_0 and λ_1 describe the interaction of an electron and a hole contribution of processes with total spin 0 and 1, respectively. The first and the second terms in Eq. (1) originate from the interaction of an electron and a hole with a zero projection of the total spin on the direction of the magnetic field ($\boldsymbol{M} = 0$), and the third and fourth terms from interactions with $\boldsymbol{M} = +1$ and $\boldsymbol{M} = -1$, respectively. In the case when the ratio $\frac{\lambda_1}{2\lambda_0}$ is from the interval $\langle -1/3,\ 0\rangle$ at zero magnetic field, the logarithmic anomaly of the first term is partially compensated by three equal logarithmic terms with opposite sign. In a finite field ($E_Z > 0$) a part of the electronic DOS at Fermi energy is removed due to spin polarization and two singularities/maxima should appear at $\pm E_Z$. Thus, due to the spin polarization in the magnetic field the logarithmic singularity/minimum at the Fermi level is more pronounced than it was in the zero-field case. The parameters $\Gamma_0 = \Gamma_\varepsilon$ and $\Gamma_1 = \Gamma_\varepsilon + \Gamma_s$ responsible for the broadening of AA logarithmic singularity in DOS are determined by the energy relaxation rate Γ_ε and the spin relaxation rate Γ_s [see Eq. (2.31) in Ref. [11]].

We use Eq. (1) to fit our field-dependent tunneling conductance data from Fig. 2(b) measured above B_{c2}. As the first step, the parameters characterizing the field-dependent AA effect $\frac{\lambda_1}{2\lambda_0}$, χ, Γ_0, and Γ_1 have been determined from the tunneling conductance measured deeply in the normal state at $B = 8\,T$ and $T = 0.5$ K. Afterwards, for the fits at lower fields, the same set of parameters was applied. Below B_{c2}, a formula which combines the Dynes DOS and the AA correction in the normal state has been used, in the form of $N(E) = N_S^D(E)N_N(\Omega)$. The latter term involves complex energy $\Omega(E) = \mathrm{Re}[\sqrt{(E + i\Gamma_D)^2 - \Delta^2}$ necessary to keep the number of charge carriers constant after the transition to the superconducting state [24]. During the fit below B_{c2} we varied the value of the energy gap Δ and slightly corrected the values of Γ_D. Since the spectra in Figs. 2(b) and 3(a) do not reveal any apparent spin splitting in the superconducting state due to large Γ_D, we use a simple Dynes formula, which at high spectral smearing is indistinguishable from the sum of two split Dynes DOS.

As can be seen in Fig. 3(a), our experimental tunneling spectra shown in cyan (above B_{c2}) and green curves (superconducting state) coincide well with the model (black lines). The values of the fitting parameters of the AA effect are $\frac{\lambda_1}{2\lambda_0} = -0.2$, $\tilde{\lambda}_0 = 0.145$. The broadening parameters Γ_D, Γ_0, and Γ_1 have about the same value $\approx$0.3 meV, which is striking and deserves further investigations. The superconducting gap $\Delta(B)$ obtained from the fit follows a square field dependence (see the Supplemental Material [14]), in agreement with the predictions of Herman and Hlubina [19] for the Zeeman splitting in Dynes superconductors with strong spectral smearing $\Gamma_D > 0.3\Delta$. Red points in Fig. 3(c) represent the magnetic field dependence of the ZBC from Fig. 2(b) and other spectra (not shown). The dashed-dotted line depicts the contribution of the Dynes model, the dashed line is the spin-dependent AA contribution, and the solid line is the combined Dynes-AA model. It is obvious that the model provides a reasonable theoretical description of the measured tunneling spectra in both the superconducting as well as the normal states.

The observation of the Zeeman-driven SIT transition in homogeneously disordered thin films in a perpendicular magnetic field is really surprising. This effect has not yet been observed possibly because there are only few experimental studies using local DOS measurements in such systems [25,26]. These works agree that the vortices are vanishing at strong disorder and the DOS in the normal state above B_{c2} is strongly reduced at the Fermi level. However, systematic studies of the reduced normal-state DOS at fields above B_{c2} in strongly disordered systems are lacking. In disordered NbN [26] the STM DOS measured in the vortex core (with a presumably normal-state DOS) features enhanced/deeper minimum in the reduced DOS than above T_c at $B = 0$. It is very similar to our case, but was neither noticed nor studied in detail. Notably, Wu *et al.* [27] have observed Zeeman splitting of the logarithmic AA DOS anomaly in the moderately disordered Al films in a parallel field attributed not to the diffusive channel as in our MoC but to the Cooper channel. It is important to study the normal-state properties of disordered superconductors at temperatures well below T_c systematically.

In summary, the tunneling spectroscopy and transport measurements of a highly disordered 3-nm thin MoC film with $k_F l$ close to unity in transverse magnetic fields exhibit the Zeeman effects which play an important role in both the superconducting state and the insulating state. In the superconducting state the superconductivity is suppressed by the paramagnetic pair breaking as witnessed by the value of B_{c2} close to the Clogston limit and also by the temperature dependence of B_{c2} (T). The features of Zeeman coupling are found in the superconducting density of states wherein by increasing the magnetic field up to B_{c2} the superconducting gap is gradually filled rather than closed, and in the case of small broadening a Zeeman splitting of the gaplike peaks is observed. In the normal state above B_{c2} the experimental data can be even quantitatively described by the AA quantum corrections: The DOS shows enhancement of the logarithmic anomaly with increasing magnetic field driving the system deeper into the insulating or resistive state. This effect is due to the spin-dependent electron-hole interaction. Consistently, a spin-dependent Altshuler-Aronov correction is also needed to explain the transport data measured above B_{c2}, in full agreement with the analysis of DOS. Thus, we can conclude that superconductor-insulator transition in a strongly disordered MoC film in a transverse magnetic field is driven by the Zeeman effects. This transition, not showing any emergent inhomogeneity in the spectral maps above B_{c2}, remains fully fermionic.

We gratefully acknowledge helpful conversations with B. L. Altshuler and R. Hlubina. The work was supported by the projects APVV-18-0358, VEGA 2/0058/20, VEGA 1/0743/19, EMP-H2020 Project No. 824109, the COST action CA16218 (Nanocohybri) and by US Steel Košice.

[1] V. F. Gantmakher and V. T. Dolgopolov, Superconductor-insulator quantum phase transition, Phys. Usp. **53**, 1 (2010).
[2] N. Trivedi, in *Conductor Insulator Quantum Phase Transitions*, edited by V. Dobrosavljevic, N. Trivedi, and J. M. Valles, Jr. (Oxford University Press, Oxford, 2012), p. 329.
[3] M. P. A. Fisher, Quantum Phase Transitions in Disordered Two-Dimensional Superconductors, Phys. Rev. Lett. **65**, 923 (1990).
[4] B. Sacépé, C. Chapelier, T. I. Baturina, V. M. Vinokur, M. R. Baklanov, M. Sanquer *et al.*, Disorder-Induced Inhomogeneities of the Superconducting State Close to the Superconductor-Insulator Transition, Phys. Rev. Lett. **101**, 157006 (2008).
[5] A. M. Finkel'stein, Superconducting transition temperature in amorphous films, Pisma Zh. Eksp. Teor. Fiz. **45**, 37 (1987) [Sov. Phys. JETP Lett. **45**, 46 (1987)].
[6] P. Szabó, T. Samuely, V. Hašková, J. Kačmarčík, M. Žemlička, M. Grajcar, J. G. Rodrigo, and P. Samuely, Fermionic scenario for the destruction of superconductivity in ultrathin MoC films evidenced by STM measurements, Phys. Rev. B **93**, 014505 (2016).
[7] V. Hašková, M. Kopčík, P. Szabó, T.Samuely, J. Kačmarčík, O. Onufriienko, M. Žemlička, P. Neilinger, M. Grajcar, and P. Samuely, On the origin of in-gap states in homogeneously disordered ultrathin films. MoC case, Appl. Surf. Sci. **461**, 143 (2018).
[8] A. Kapitulnik, S. A. Kivelson, and B. Spivak, Colloquim: Anomalous metals: Failed superconductors, Rev. Mod. Phys. **91**, 011002 (2019).
[9] C. Yang, Y. Liu, Y. Wang, L. Feng, Q. He, J. Sun, Y. Tang, C. Wu, J. Xiong, W. Zhang *et al.*, Intermediate bosonic metallic states in the superconductor-insulator transition, Science **366**, 1505(2019).
[10] B. L. Altshuler, A. G. Aronov, and P. A. Lee, Interaction Effects in Disordered Fermi Systems in Two Dimensions, Phys. Rev. Lett. **44**, 1288 (1980).
[11] B. L. Altshuler and A. G. Aronov, in *Electron-Electron Interactions in Disordered Systems*, edited by A. L. Efros and M. Pollak, Modern Problems in Condensed Matter Sciences Vol. 10 (Elsevier Science/North-Holland, New York, 1985), p. 1.
[12] M. Trgala, M. Žemlička, P. Neilinger, M. Rehák, M. Leporis, Š. Gaži, J. Greguš, T. Pleceník, T. Roch, E. Dobročka, and M. Grajcar, Superconducting MoC thin films with enhanced sheet resistance, Appl. Surf. Sci. **312**, 216 (2014).
[13] E. L. Haase, Preparation and characterization of MoC_x thin films, J. Low Temp. Phys. **69**, 246 (1987).
[14] See Supplemental Material at http://link.aps.org/supplemental/10.1103/PhysRevB.102.180508 for more detailed information about the correlation studies of superconducting and normal state properties with surface corrugations, determination of the upper critical magnetic field from transport and tunneling measurements and theoretical description of the normal state transport data.
[15] Y. Matsuda and H. Shimahara, Fulde-Ferrell-Larkin-Ovchinnikov state in heavy fermion superconductors, J. Phys. Soc. Jpn. **76**, 051005 (2007).
[16] A. Larkin and A. Varlamov, *Theory of Fluctuations in Superconductors* (Oxford University Press, New York, 2005).
[17] V. Galitski and A. Larkin, Superconducting fluctuations at low temperature, Phys. Rev. B **63**, 174506 (2001).
[18] R. C. Dynes, V. Narayanamurti, and J. P. Garno, Direct Measurement of Quasiparticle-Lifetime Broadening in a Strongly-Coupled Superconductor, Phys. Rev. Lett. **41**, 1509 (1978).
[19] F. Herman and R. Hlubina, Microscopic interpretation of the Dynes formula for the tunneling density of states, Phys. Rev. B **94**, 144508 (2016).
[20] S. Bogdanovich, P. Dai, M. P. Sarachik, and V. Dobrosavljevic, Universal Scaling of the Magnetoconductance of Metallic Si:B, Phys. Rev. Lett. **74**, 2543 (1995).
[21] R. Meservey and P. Fulde, Magnetic Field Splitting of the Quasiparticle States in Superconducting Aluminum Films, Phys. Rev. Lett. **25**, 1270 (1970).
[22] A. M. Clogston, Upper Limit for the Critical Field in Hard Superconductors, Phys. Rev. Lett. **9**, 266 (1962).
[23] P. Neilinger, J. Greguš, D. Manca, B. Grančič, M. Kopčík, P. Szabó, P. Samuely, R. Hlubina, and M. Grajcar, Observation of quantum corrections to conductivity up to optical frequencies, Phys. Rev. B **100**, 241106(R) (2019).
[24] R. Hlubina (private communication).
[25] I. Roy, R. Ganguly, H. Singh, and P. Raychaudhuri, Robust pseudogap across the magnetic field driven superconductor to insulator-like transition in strongly disordered NbN films, Eur. Phys. J. B **92**, 49 (2019).
[26] Y. Noat, V. Cherkez, C. Brun, T. Cren, C. Carbillet, F. Debontridder, K. Ilin, M. Siegel, A. Semenov, H.-W. Hübers, and D. Roditchev, Unconventional superconductivity in ultrathin superconducting NbN films studied by scanning tunneling spectroscopy, Phys. Rev. B **88**, 014503 (2013).
[27] W. Wu, J. Williams, and P. W. Adams, Zeeman Splitting of the Coulomb Anomaly: A Tunneling Study in Two Dimensions. Phys. Rev. Lett. **77**, 1139 (1996).

Correction: A minor error in the displayed equation below Eq. (1) has been fixed.